Gold Nanotubes with a Nanoporous Wall: Their Ultrathin Platinum Coating and Superior Electrocatalytic Activity toward Methanol Oxidation

Tae-Yeon Shin, Sang-Hoon Yoo, and Sungho Park*

Department of Chemistry, BK21 School of Chemical Materials Science & SKKU Advanced Institute of Nanotechnology, Sungkyunkwan University, Suwon 440-746, South Korea

Received March 25, 2008. Revised Manuscript Received May 23, 2008

This paper describes a new strategy for synthesizing hollow nanotubes (pore $d > 100$ nm) with nanoporous walls (pore $d < 10$ nm) as well as how the nanoporous hollow nanotubes exhibit better intrinsic electrocatalytic activity toward methanol oxidation compared with an analogous nanotube system with smooth walls. Compared with vertical arrays of a nanorod system, the nanotube system is better in terms of increasing the effective surface area because the inner and outer surfaces are both in contact with the reaction medium. Au nanotubes with smooth wall and nanoporous walls were synthesized using AAO and conducting polymer nanorod templates. The surface of Au nanotube walls could be electrochemically coated with ultrathin Pt layers without changing the nanoporous structure. The resulting nanotubes showed different "intrinsic" electrocatalytic activities toward methanol oxidations depending on the wall structure (smooth or nanoporous). We compared its catalytic activity with the commercially available carbon-supported Pt nanoparticles and found that the catalytic activity of nanoporous nanotubes is the best among the investigated samples. The reason for this superior catalytic activity was attributed to the higher CO-poisoning tolerance and shorter effective length for electronic transportation.

1. Introduction

Understanding how the catalytic and adsorptive/desorptive properties of metal surfaces depend on their crystallographic structure, size, and local environment is an intriguing issue in surface chemistry. Platinum group nanoparticles (i.e., Pt, Pd, Ru, and so on) are key materials worthy of a detailed examination in methanol-air fuel cells on account of their superior catalytic activity to the oxidation of methanol fuel.[1−3] Synthesizing Pt group metals in nanoparticle form offers a high surface area for high catalytic activity and utilization efficiency.[3−10] However, nanoparticles need to be supported on a solid substrate, such as carbon, in order to prevent their irreversible aggregation by limiting their translational freedom. In electrocatalysis, the use of support materials can create a potential problem with charge transport due to grain boundaries between the supporting materials. Therefore, the formation of a continuous network with minimal grain boundaries might be beneficial to the increase of electronic transportation efficiency. A nanoporous network of Pt metals was suggested as one example to solve these problems.[11] A bimodal pore size distribution with large ($d >$ hundreds of nanometers) and small pores ($d <$ tens of nanometers) for reactant accessibility and high surface area, respectively, is useful for electrocatalytic nanoporous materials.[12] Previously, we suggested that vertical nanoporous nanorods arrays could meet this requirement.[13] This paper describes a new strategy for synthesizing hollow nanotubes (pore $d > 100$ nm) with nanoporous walls (pore $d < 10$ nm) as well as how the nanoporous hollow nanotubes exhibit better intrinsic electrocatalytic activity toward methanol oxidation compared with an analogous nanotube system with smooth walls. Compared with vertical arrays of a nanorod system, the nanotube system is better in terms of increasing the effective surface area because the inner and outer surfaces are both in contact with the reaction medium.

2. Experimental Section

A thin layer of gold (∼1 μm) was thermally evaporated onto one side of a nanoporous anodic alumina membrane (pore size =

* Corresponding author. E-mail: spark72@skku.edu. Fax: 82-31-290-7075.

(1) *Interfacial Electrochemistry*; Wieckowski, A., Ed.; Marcel Dekker: New York, 1999.
(2) *Electrocatalysis*; Lipkowski, J., Ross, P. N., Eds.; Wiley-VCH: New York, 1998.
(3) Park, S.; Wieckowski, A.; Weaver, M. J. *J. Am. Chem. Soc.* **2003**, *125*, 2282.
(4) Carrette, L.; Friedrich, K. A.; Stimming, U. *ChemPhysChem* **2000**, *1*, 162.
(5) Tong, Y. Y.; Kim, H. S.; Babu, P. K.; Waszczuk, P.; Wieckowski, A.; Oldfield, E. *J. Am. Chem. Soc.* **2002**, *124*, 468.
(6) Horswell, S. L.; O'Neil, I. A.; Schiffrin, D. J. *J. Phys. Chem. B* **2001**, *105*, 941.
(7) Park, S.; Wasileski, S.; Weaver, M. J. *J. Phys. Chem. B* **2001**, *105*, 9719.
(8) Mukerjee, S.; McBreen, J. *J. Electroanal. Chem.* **1998**, *448*, 163.
(9) Ganesan, R.; Lee, J. S. *Angew. Chem., Int. Ed.* **2005**, *44*, 6557.
(10) Hull, R. V.; Li, L.; Xing, Y.; Chusuei, C. C. *Chem. Mater.* **2006**, *18*, 1780.
(11) Hu, Y.-S.; Guo, Y.-G.; Sigle, W.; Hore, S.; Balaya, P.; Maier, J. *Nat. Mater.* **2006**, *5*, 713.
(12) Ding, Y.; Erlebacher, J. *J. Am. Chem. Soc.* **2003**, *125*, 7772.
(13) Yoo, S.-H.; Park, S. *Adv. Mater.* **2007**, *19*, 1612.
(14) Erlebacher, J.; Aziz, M. J.; Karma, A.; Dimitrov, N.; Sieradzki, K. *Nature* **2001**, *410*, 450.
(15) Park, S.; Yang, P.; Corredor, P.; Weaver, M. J. *J. Am. Chem. Soc.* **2002**, *124*, 2428.
(16) Yoo, S.-H.; Park, S. *Electrochim. Acta* **2008**, *53*, 3656.
(17) Park, S.; Xie, Y.; Weaver, M. J. *Langmuir* **2002**, *18*, 5792.

10.1021/cm800859k CCC: $40.75
Published on Web 09/02/2008

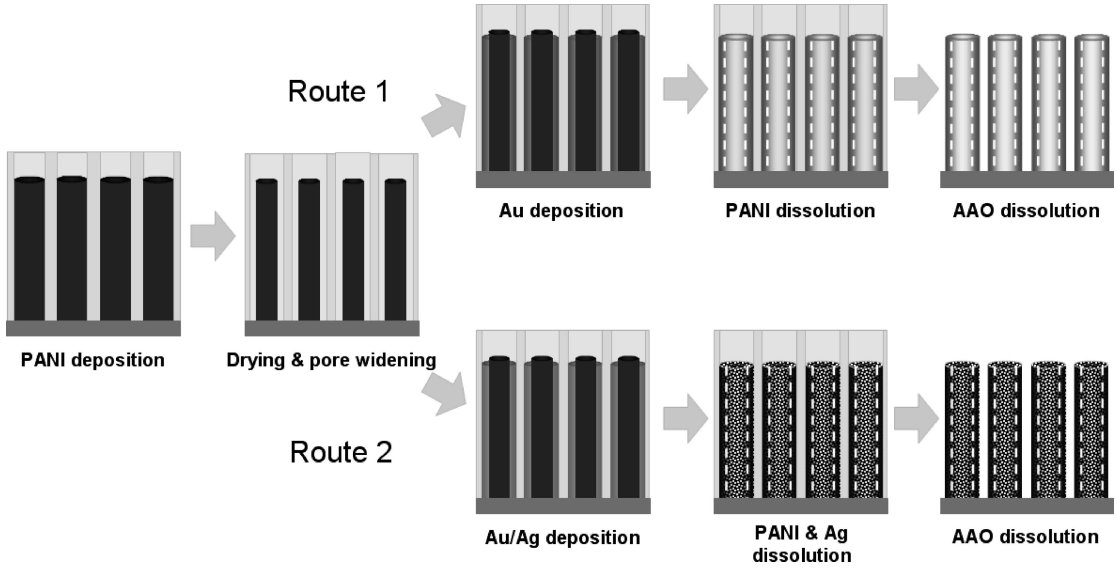

Figure 1. Schematic representation of the experimental procedure for the synthesis of NTs with smooth walls (route 1) and with nanoporous walls (route 2).

250−350 nm, from Whatman Inc.), which served as the working electrode in a three electrode system after making physical contact with a glassy carbon electrode. A Pt wire and Ag/AgCl electrode were used as the counter and reference electrode, respectively.[18−20] Conducting polyaniline (PANI) nanorods (NRs) were grown electrochemically into the interior of an anodic alumina template by potential cycling for 80 times between −0.2 and +1.2 V (vs Ag/AgCl) at a sweep rate of 100 mV/s, from a solution of aniline in H_2SO_4 (0.1 M aniline, 0.5 M H_2SO_4, in water). The length of the PANI NRs were controlled by monitoring the charge that passed through the cell during electrodeposition. After deposition, the film was dried at 80 °C to induce the diameter contraction. Au (from Technic Inc.) was then deposited into the empty space between a PANI NR and the wall of AAO, which is similar to a previously published report.[21] PANI NRs were dissolved in concentrated nitric acid and the AAO membrane was dissolved in a 3 M sodium hydroxide solution. Gold/silver alloy nanoshells were electrodeposited from a solution containing gold/silver ions (mole ratio, Au^+:Ag^+ = 1:3, 0.25 mL of 0.05 M $KAu(CN)_2$ and 0.25 M Na_2CO_3 solution was mixed with 0.75 mL of 0.05 M $KAg(CN)_2$ and 0.25 M Na_2CO_3 solution) in basic cyanide solutions, at a constant potential of −0.95 V.[22] The Cu upd layer was formed by holding the potential at 0.1 V for 100 s in 0.1 M H_2SO_4 as the supporting electrolyte containing Cu ions (0.01 M $CuCl_2$). An aqueous solution containing 5 mM $H_2PtCl_6 \cdot nH_2O$ (n = 5.7) as the Pt ion source was used in the Cu upd layer replacement reactions.[15] All the replacement reactions were carried out by immersing the Cu upd layer coated Au NT arrays into a solution containing Pt metal ions for 10 min at room temperature. FESEM and TEM images were obtained using JEOL 7000F and JEOL JEM-3011, respectively. The electrode potentials were measured and referenced to an Ag/AgCl (sat. KCl) reference electrode (from Autolab AUT12, and Bioanalytical Systems, respectively). A Pt wire was used as a counter electrode for all the experiments. For Pt/C nanoparticle immobilization, we adopted the previously reported methods.[3,7,17]

3. Results and Discussion

Porous metallic materials, especially nanoporous gold, have received increasing attention because of their interesting catalytic behaviors in catalysis as well as high surface area in the given geometrical surface are.[23−26] Nanoporous gold film was fabricated either by electrochemical deposition or dealloying process.[23−26] Herein, we describe how one can fabricate three-dimensional nanoporous Au nanotube arrays and an ultranthin layer of Pt coating on such architectures.

Figure 1 shows a schematic diagram of the synthetic process for nanotubes (NTs) with smooth and nanoporous walls. Electrochemically grown polyaniline (PANI) nanorods (NRs) were predeposited into the interior of an anodized aluminum oxide (AAO) membrane and used as a template for Au NT formation. This procedure generated an array of vertically aligned Au NTs with smooth walls. A similar procedure was used for the synthesis of Au NT arrays with nanoporous walls. Gold/silver alloy nanoshells were electrodeposited from a gold/silver ion (mole ratio, Au^+:Ag^+ = 1:3) solution in basic cyanide solutions. Nanoporous walls were generated from dealloying (selective dissolution of less noble metal) gold/silver alloy shells with concentrated nitric acid that also dissolved the contained PANI NRs. The porous architecture formed due to an intrinsic dynamic pattern formation process, in which the more noble metal (Au) atoms tend to aggregate into two-dimensional clusters through a phase separation process at the solid−acid interface.[14] Images A and B in Figure 2 show typical scanning electron microscopy (SEM) images of the vertical arrays of bare Au NTs with smooth and nanoporous walls, respectively. The length, average inner diameter and wall thickness of the Au NTs with smooth walls was 4 (± 0.16 μm), 196 (± 33 nm), and 62 (± 18 nm), respectively. The Au NTs with nanopo-

(18) Park, S.; Lim, J.-H.; Chung, S.-W.; Mirkin, C. A. *Science* **2004**, *303*, 348.
(19) Qin, L.; Park, S.; Huang, L.; Mirkin, C. A. *Science* **2005**, *309*, 113.
(20) Martin, C. R. *Science* **1994**, *266*, 1961.
(21) Lahav, M.; Weiss, E. A.; Xu, Q.; Whitesides, G. M. *Nano Lett.* **2006**, *6*, 2166.
(22) Ji, C.; Searson, P. C. *J. Phys. Chem. B* **2003**, *107*, 4494.
(23) Jia, F.; Yu, C.; Ai, Z.; Zhang, L. *Chem. Mater.* **2007**, *19*, 3648.
(24) Zhang, J.; Liu, P.; Ma, H.; Ding, Y. *J. Phys. Chem. C* **2007**, *111*, 10382.
(25) Yu, C.; Jia, F.; Ai, Z.; Zhang, L. *Chem. Mater.* **2007**, *19*, 6065.
(26) Huang, J.-F.; Sun, I.-W. *Adv. Funct. Mater.* **2005**, *15*, 989.

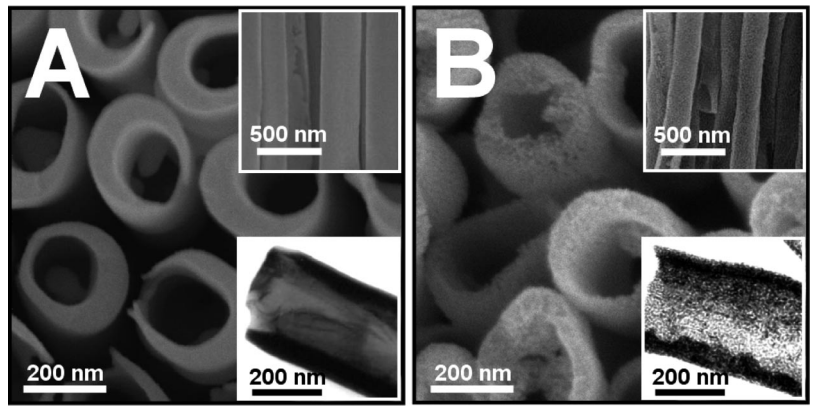

Figure 2. Field-emission SEM images. Vertical Au NT arrays with (A) smooth and (B) nanoporous walls. Upper insets show the side view for each sample. Lower insets show the corresponding TEM images.

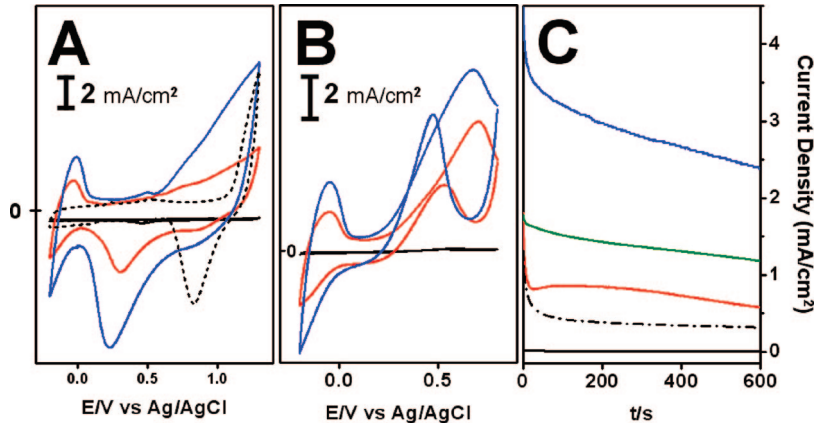

Figure 3. (A) Cyclic voltammograms (50 mV s^{-1}) for a flat Pt plate (black solid line), Au NTs with smooth walls (red traces), and Au NTs with nanoporous walls (blue traces) after ultrathin Pt layer coating. Lengths ≈ 4 (± 0.16 μm) and the geometrical surface area ≈ 1 cm^2. Black dashed traces is for bare Au NTs with nanoporous walls. (B) Cyclic voltammograms (50 mV s^{-1}) for electrooxidation of 0.1 M methanol in 0.1 M H_2SO_4 on the same corresponding samples shown in A. (C) Current density−time curves recorded at 0.4 V (vs Ag/AgCl) in 0.1 M methanol and 0.1 M H_2SO_4, on a flat Pt plate (black traces), Pt/C (60% Pt loading) nanoparticles (black-dashed-dot traces), NTs with smooth walls (red traces, $L \approx 4$ μm), NTs with nanoporous walls (green traces, $L \approx 1.7$ μm), and NTs with nanoporous walls (blue traces, $L \approx 4$ μm). The current scale given is normalized in each case to a 1 cm^2 Pt "geometrical area".

rous walls showed similar physical dimensions to those with smooth walls, and had a nanopore diameter of 7 (± 2 nm).

These synthesized NT arrays can be utilized as a template for producing ultrathin Pt layers coating to convert electrocatalytically inactive Au NTs into active electrocatalysts. In this way, the Au NT architecture serves as a support with a continuous network and the electrocatalytically active metal, such as Pt, resides mainly on the surface, which maximized the use of catalytically active metals. The ultrathin Pt layer coating was achievable on the Au surface through copper under-potential-deposition (upd), followed by the spontaneous replacement with the nobler Pt metal ions. Previously, this method was applied to synthesizing Au/Pt core/shell nanoparticles and NR arrays.[15,16] The advantage of this strategy is that the morphology of the nanoporous walls can be retained without plugging the fine structure. There were no morphological changes in the Au NTs before and after Pt layer coating. Energy-dispersive X-ray spectroscopy (EDS) elemental mapping showed 4.5% of Pt on these structures, which represents an ultrathin Pt layer coating (see the Supporting Information, Figure S1). The cyclic voltammograms (CV) provide clear evidence that the Au NT surface had been modified entirely by Pt metal, as shown in Figure 3A. Figure 3A shows representative CVs obtained (at 50 mV/s) from −0.2 to 1.3 V vs Ag/AgCl for the Au NT arrays with smooth and nanoporous walls in 0.1 M sulfuric acid. The cathodic removal of Au oxide at 0.8 V in the negative scan direction is a well-known feature of bare Au electrochemistry, which is absent after Pt layer coating in Figure 3A. Instead, there are broad peaks from 0.0 V to −0.2 V, which is indicative of the cathodic−anodic current profile associated with hydrogen adsorption and desorption on a Pt surface. The presence of a Pt oxide reduction peak at ca. 0.3 V in the negative scan direction also indicates the homogeneous Pt coating on the Au NTs without any Au pinholes. When the lengths of the NTs are similar (both are ca. 4 μm), the NTs with nanoporous walls show an approximately 2 fold higher Pt oxide reduction peak area than the NTs with smooth walls. The peak area is proportional to the exposed surface area of Pt. A similar estimation could be obtained from hydrogen adsorption/desorption peak area analysis. As a comparison, the CV of the flat Pt substrate is presented as black solid line, which has one sixtieth of peak area of NTs with nanoporous walls in the same geometrical area. This demonstrates that the vertical array of a quasi-one-dimensional structure is an efficient route for achieving a high surface area in a given geometrical area. Furthermore, fine control of the wall morphology by endow-

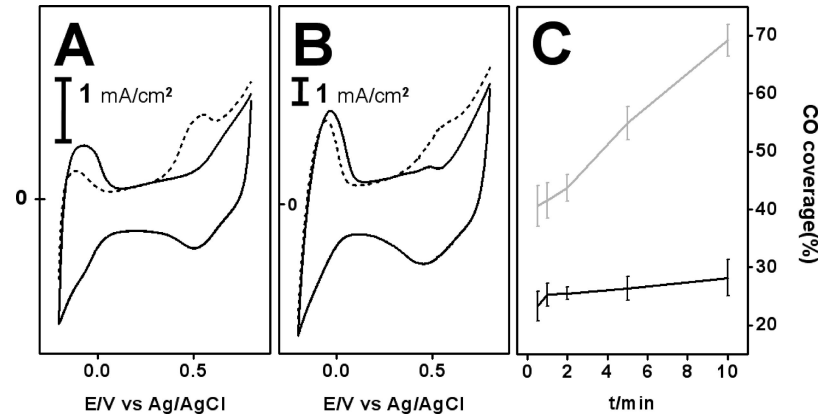

Figure 4. Cyclic voltammograms (50 mV s^{-1}) for removal of adsorbed species (mainly CO) following exposure of (A) NTs with smooth walls and (B) NTs with nanoporous walls to 0.1 M methanol in 0.1 M H_2SO_4 at 0 V for 10 min and subsequent solution flushing with supporting electrolyte (dashed traces). The solid traces are corresponding cyclic voltammograms obtained after adsorbate removal. Length of both NTs ≈ 4 (± 0.16 μm). (C) Immersion time versus CO-coverages on NTs with smooth walls (gray traces) and on NTs with nanoporous walls (black traces). The current scale given is normalized in each case to a 1 cm^2 Pt "geometrical area".

ing a nanoporous architecture is another way of further increasing the surface area. Arrays of NTs have advantages regarding mass transport by providing hollow channels for each NT. A bimodal pore size distribution, larger pores (d > hundreds of nanometers) for reactant accessibility and small pores (d < tens of nanometers) for high surface area, is highlighted by the resulting NTs with nanoporous walls.

The electrocatalytic activity of the resulting NTs for methanol oxidation was measured in an electrolyte containing 0.1 M methanol and 0.1 M H_2SO_4 using CVs, as shown in Figure 3B. The peak potential for the oxidation of methanol is approximately 0.7 and 0.5 V for the positive and the negative scan directions, respectively. These values are in good agreement with the values reported in the literature.[17] The current density-time curves measured at a fixed potential were used to test the steady-state performance in the oxidation of methanol at room temperature. Figure 3C shows the current densities measured at 0.4 V (vs Ag/AgCl) in a solution containing 0.1 M methanol in 0.1 M H_2SO_4. As is well-known, the high initial current originates from double-layer charging. The current density decreased sharply within the first few seconds and reached a pseudosteady state. The NTs with nanoporous walls showed the highest activity among the samples investigated. As a comparison, one representative sample, which is commercially available carbon-supported Pt (C/Pt) nanoparticles (Pt mass content ~60% (average nanoparticle diameter ~8.8 nm) from E-TEK) was also examined under the same experimental conditions and their current densities were normalized by controlling the amount of C/Pt nanoparticles to have the same effective area as the NTs ($L \approx 4$ μm) with smooth walls for a direct comparison (black-dashed-dot traces in Figure 3C). This current normalization procedure allows a comparison of their "intrinsic" electrocatalytic activities. As shown in Figure 3C, the electrocatalytic activity of Pt/C nanoparticles was better than the activity of the Pt plates but worse than the activity of our NTs. The current density of the NTs with nanoporous walls was ca. 2.8 mA/cm^2 at 600s. In contrast, the NTs with the smooth walls and the flat Pt substrate was 0.8 and 0.005 mA/cm^2 at 600s, respectively. By considering the effective surface area of those substrates (from the hydrogen adsorption/desorption charges), the NTs with nanoporous walls have an effective surface area of 285 cm^2. This number was obtained from the hydrogen desorption charge on a polycrystalline Pt surface, which is 240 μC/cm^2. The NTs with smooth walls showed an effective surface area of 143 cm^2. Therefore, the NTs with nanoporous walls can have approximately 2 times larger surface area than the NTs with smooth walls. However, the measured current density with nanoporous walls is higher than the expected value from the surface area considerations. In order to clarify this point, the NTs with nanopores having the same effective surface area with NTs with smooth wall were synthesized. Comparable surface area to the NTs smooth walls was obtained when the length of the NTs with nanopores was reduced to 1.7 (± 0.13 μm). The green traces in Figure 3C clearly exhibit the superior catalytic activity of the NTs with the nanopores over the NTs with smooth surfaces. One of possible reason for this is related to the degree of tolerance toward poisoning by CO-like intermediates. It is well-known that Pt sites are progressively deactivated by the CO-like intermediates formed during the dissociation process of methanol. As a means of assaying the extent of chemisorbed CO-like intermediate formation under reaction conditions for each system, CVs were measured after removing the methanol by repeated flushing with the supporting electrolyte while holding the potential at a fixed value. This tactic has been used to measure the coverage of CO-like species on Pt nanoparticles as a function of the particle size.[17] Approximate estimates of the fractional CO-like species coverage, θ_{CO} (where saturation is regarded as $\theta_{CO} = 1$), were obtained from the extent to which the hydrogen adsorption/desorption charge (in the -0.2 to 0.1 V region) is attenuated relative to the complete removal of CO species.[17] A previous analysis of Pt nanoparticles showed that the production of CO-like species production decreased with decreasing nanoparticle size.[17] As shown in panels A and B of Figure 4, the NTs with nanopores showed higher tolerance toward CO-poisoning than the NTs with smooth walls. Under the given experimental conditions (0.1 M methanol in 0.1 M H_2SO_4 held at 0 V for 10 min), the porous NTs showed a $\theta_{CO} =$

0.28 but the smooth NTs showed a $\theta_{CO} = 0.70$. Figure 4C clearly shows the better tolerance of porous NTs toward CO poisoning than the analogous smooth NTs within the time period examined. Therefore, there is an intrinsic difference in methanol oxidation between the smooth and nanoporous NTs, which can be attributed to the difference in CO tolerance depending on the morphology of the wall structure. As indicated with Pt nanoparticle systems,[17] the smaller θ_{CO} from the dissociation of methanol on the surface of nanopores can be attributed to the decreasing availability of continuous terrace binding sites, assuming that C−H bond cleavage is facilitated by the availability of an adjacent Pt site to bind a H atom. The relative ineffectiveness of such sites for methanol dissociation with NTs with nanopore walls is expected, even though there is no direct method for measuring the distribution of continuous Pt sites on nanopores.

The electrochemical performance and the morphological change of nanoporous NTs were tested with repeated potential cycling (100 cycles) from −0.2 to +0.8 V with a scan rate of 50 mV s^{-1} for electrooxidation of 0.1 M methanol in 0.1 M H_2SO_4. There were no dramatic catalytic activities or morphological changes with nanoporous NTs before and after potential cycling, as shown in Figure 5. Previously, it was shown that the surface modification of nanoporous bulk Au film with Pt was helpful in terms of reserving the structural integrity of nanopores structure.[24]

4. Conclusion

In conclusion, these results show that the morphology control of nanostructures is important for synthesizing highly efficient electrocatalysts. A dual size distribution, i.e., the formation of vertical arrays of hollow NTs and the fine structures such as nanopores on the wall of NTs, is important not only for generating a high surface area and easy transport of reactants but also for the fine-tuning of intrinsic catalytic activities. There are many routes for achieving a dual size distribution. As shown in this study, the hierarchical fine-control of nanostructures will make an important impact in advancing nanoparticle related applications such as electrocatalysis, sensors, and surface wettability.

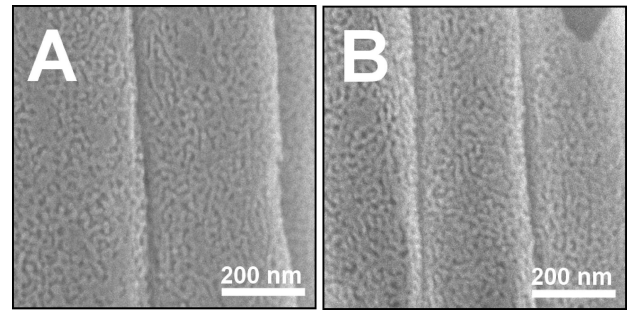

Figure 5. FESEM images of nanoporous Au NTs with ultrathin Pt coating (A) before and (B) after repeated 100 potential cyclings from −0.2 to +0.8 V with a scan rate of 50 mV s^{-1} for electrooxidation of 0.1 M methanol in 0.1 M H_2SO_4.

Acknowledgment. This study was supported by the Korea Research Foundation Grant funded by the Korean Government (MOEHRD, KRF-2005-005-J11902, and KRF-C00050) and the Korea Science and Engineering Foundation (R01-2006-000-10426-0-2006).

Supporting Information Available: EDS analysis (PDF). This material is available free of charge via the Internet at http://pubs.acs.org.

CM800859K